



SIRT1 inhibits NADPH oxidase activation and protects endothelial function in the rat aorta: Implications for vascular aging



María José Zarzuelo^{a,1}, Rocío López-Sepúlveda^{a,1}, Manuel Sánchez^a, Miguel Romero^a, Manuel Gómez-Guzmán^a, Zoltan Ungvary^b, Francisco Pérez-Vizcaíno^c, Rosario Jiménez^a, Juan Duarte^{a,*}

^a Department of Pharmacology, School of Pharmacy, University of Granada, 18071 Granada, Spain

^b Reynolds Oklahoma Center on Aging, Department of Geriatric Medicine, University of Oklahoma, Oklahoma, USA

^c Department of Pharmacology, School of Medicine, University Complutense of Madrid and Ciber Enfermedades Respiratorias (CIBERES), Madrid, Spain

ARTICLE INFO

Article history:

Received 18 December 2012

Accepted 11 February 2013

Available online 17 February 2013

Keywords:

SIRT1
Endothelial dysfunction
NADPH oxidase
PPAR α

ABSTRACT

Vascular aging is characterized by up-regulation of NADPH oxidase, oxidative stress and endothelial dysfunction. Previous studies demonstrate that the activity of the evolutionarily conserved NAD⁺-dependent deacetylase SIRT1 declines with age and that pharmacological activators of SIRT1 confer significant anti-aging cardiovascular effects. To determine whether dysregulation of SIRT1 promotes NADPH oxidase-dependent production of reactive oxygen species (ROS) and impairs endothelial function we assessed the effects of three structurally different inhibitors of SIRT1 (nicotinamide, sirtinol, EX527) in aorta segments isolated from young Wistar rats. Inhibition of SIRT1 induced endothelial dysfunction, as shown by the significantly reduced relaxation to the endothelium-dependent vasodilators acetylcholine and the calcium ionophore A23187. Endothelial dysfunction induced by SIRT1 inhibition was prevented by treatment of the vessels with the NADPH oxidase inhibitor apocynin or superoxide dismutase. Inhibition of SIRT1 significantly increased vascular superoxide production, enhanced NADPH oxidase activity, and mRNA expression of its subunits p22^{phox} and NOX4, which were prevented by resveratrol. Peroxisome proliferator-activated receptor- α (PPAR α) activation mimicked the effects of resveratrol while PPAR α inhibition prevented the effects of this SIRT1 activator. SIRT1 co-precipitated with PPAR α and nicotinamide increased the acetylation of the PPAR α coactivator PGC-1 α , which was suppressed by resveratrol. In conclusion, impaired activity of SIRT1 induces endothelial dysfunction and up-regulates NADPH oxidase-derived ROS production in the vascular wall, mimicking the vascular aging phenotype. Moreover, a new mechanism for controlling endothelial function after SIRT1 activation involves a decreased PGC-1 α acetylation and the subsequent PPAR α activation, resulting in both decreased NADPH oxidase-driven ROS production and NO inactivation.

© 2013 Elsevier Inc. All rights reserved.

1. Introduction

Endothelial function declines with age [1–5]. The decline in endothelium-dependent dilatation is predictive of future cardiovascular events in older adults without previous disease [6,7]. A reduced bioavailability of endothelium-derived nitric oxide (NO) as a result of increased NO degradation by superoxide anion (O₂^{•-}) has been implicated as a major mechanism for age-related endothelial dysfunction [8–15]. In fact, NAD(P)H oxidase-derived reactive oxygen species (ROS) contribute to impaired endothelium-dependent dilation in arteries from old rats [16] and humans

[17]. Similarly, exogenous antioxidants improve vasodilation [18] and exercise hyperemia [19] in the aged human forearm vasculature. Thus, understanding the mechanisms regulating eNOS, ROS and NO-mediated endothelium-dependent dilation with aging has important implications for age-associated cardiovascular disease.

Several signaling pathways have been reported to mediate and/or modulate the effects of caloric restriction (CR) on aging. A number of individual components of these pathways have been validated as targets for drug development through genetic manipulation studies in animal models. One intriguing target to emerge from such studies is SIRT1, a mediator of CR effects that has been placed at a regulatory crossroad between nutrient sensing, energy metabolism and genome stability [20–23]. SIRT1 is one of seven mammalian sirtuins, a conserved family of nicotinamide adenine dinucleotide (NAD)-dependent deacetylases and

* Corresponding author. Tel.: +34 958241791; fax: +34 958248264.
E-mail address: jmduarte@ugr.es (J. Duarte).

¹ Both authors contributed equally to this paper.

ADP-ribosyltransferases that were named for the founding member, the *Saccharomyces cerevisiae* Sir2 protein (Silent information regulator 2). Deletion of Sir2 in lower organisms appears to interfere with the beneficial effects of CR in some experimental settings [24–26], although Sir2-independent lifespan extension in response to CR has also been demonstrated in yeast and worms [27,28].

SIRT1 is an unusual target for drug development because, in addition to its possible role in lifespan modulation through CR-like pathways, it exerts many other actions and effects that are relevant to health. These include promoting insulin sensitivity, modulating circadian rhythms, improving genome stability, suppressing tumors, reducing inflammation, protecting from neurodegenerative diseases, and even controlling anxiety in mice [29].

Previous studies suggest that SIRT1 activation confers vaso-protection in aged rodents. In aorta from older mice, both protein expression of SIRT1 and eNOS phosphorylation at serine 1177 were lower and acetylated eNOS were higher as compared to young mice [30–32]. Recent evidence suggests that SIRT1 promotes endothelium-dependent vascular relaxation and, conversely, downregulation of SIRT1 can impair NO-dependent endothelium-dependent dilation [33]. The mechanism by which SIRT1 regulates endothelial function is thought to operate via deacetylation of lysines 496 and 506 in eNOS [33]. On the other hand, reducing SIRT1 activity by both silencing SIRT1 [34,35] or by pharmacological inhibition [36] resulted in an increased ROS production and NADPH oxidase subunits overexpression in vascular cells. However, the role of ROS in the modulation of endothelial function by SIRT1 has not been addressed.

The present study was designed to test the hypothesis that dysregulation of SIRT1 promotes NADPH oxidase-dependent production of ROS and impairs endothelial function in the rat aorta, mimicking the vascular aging phenotype. To achieve that goal we assessed the effects of three structurally different inhibitors of SIRT1 on endothelium-dependent relaxation, vascular ROS production and NADPH oxidase activity in aorta segments isolated from young male Wistar rats.

2. Materials and methods

2.1. Tissue preparation and measurement of tension

The investigation conforms with the Guide for the Care and Use of Laboratory Animals published by the US National Institutes of Health (NIH Publication No. 85-23, revised 1996) and with the principles outlined in the Declaration of Helsinki and approved by our institutional review board. Male Wistar rats (250–300 g), obtained from Harlam Laboratories SA (Barcelona, Spain), were euthanized by a quick blow on the head followed by exsanguination. The descending thoracic aortic rings were dissected and incubated in Krebs solution (composition in mM: NaCl, 118; KCl, 4.75; NaHCO₃, 25; MgSO₄, 1.2; CaCl₂, 2; KH₂PO₄, 1.2; and glucose, 11) at 37 °C and gassed with 95% O₂ and 5% CO₂ for 5 h in a cell culture incubator in the absence or presence of nicotinamide (NAM, 1 mM) (Sigma–Aldrich, Madrid, Spain), or sirtinol (30 μM) (Sigma–Aldrich, Madrid, Spain), both of them SIRT1 and SIRT2 inhibitors, or the selective SIRT1 inhibitor EX527 (10 μM) (Tocris Bioscience, Bristol, UK), and in the presence of the SIRT1 activator resveratrol (100 μM) (Sigma–Aldrich, Madrid, Spain), the NADPH oxidase inhibitor apocynin (100 μM) (Sigma–Aldrich, Madrid, Spain), the mitochondrial complex I inhibitor rotenone (5 μM) (Sigma–Aldrich, Madrid, Spain), the peroxisome proliferator-activated receptor-α (PPARα) agonist clofibrate (1 μM) (Sigma–Aldrich, Madrid, Spain), and resveratrol plus the PPARα antagonist GW6471 (1 μM) (Tocris Bioscience, Bristol, UK). Rings were then mounted in organ chambers filled with Krebs solution and were

stretched to 2 g of resting tension by means of two L-shaped stainless-steel wires inserted into the lumen and attached to the chamber and to an isometric force-displacement transducer (Letigraph 2000, Letica S.A., Barcelona, Spain), respectively, as described previously [37], and equilibrated for 60–90 min. After equilibration, rings with endothelium were stimulated by a single concentration of phenylephrine (Phe, 1 μM) (Sigma–Aldrich, Madrid, Spain) and a concentration–response curve was constructed by cumulative addition of acetylcholine (ACh) (Sigma–Aldrich, Madrid, Spain). The concentration–relaxation response curves to sodium nitroprusside (10^{−9} M to 10^{−6} M) (Sigma–Aldrich, Madrid, Spain) were performed in the dark in rings without endothelium pre-contracted by 10^{−6} M Phe. In the case of NAM after stimulation with phenylephrine (1 μM) a concentration–response curve was also constructed by cumulative addition of the calcium ionophore (A23187) (Sigma–Aldrich, Madrid, Spain). The protocol using ACh was repeated adding superoxide dismutase (SOD, 100 U/ml) (Sigma–Aldrich, Madrid, Spain) to the organ chamber 30 min before the addition of phenylephrine.

2.2. SIRT1 activity

In order to validate the pharmacological tools and the protocol employed in the present study, the acetylation of histone-3 was studied as a measure of SIRT1 activity using Western blot.

2.3. NADPH oxidase activity

The lucigenin-enhanced chemiluminescence assay was used to determine NADPH oxidase activity in intact aortic rings, as previously described [37]. Aortic rings from all experimental groups were incubated for 30 min at 37 °C in HEPES-containing physiological salt solution (pH 7.4) of the following composition (in mM): NaCl 119, HEPES 20, KCl 4.6, MgSO₄ 1, Na₂HPO₄ 0.15, KH₂PO₄ 0.4, NaHCO₃ 1, CaCl₂ 1.2 and glucose 5.5. Aortic production of O₂^{•−} was stimulated by addition of NADPH (100 μM). Rings were then placed in tubes containing physiological salt solution, with or without NADPH, and lucigenin was injected automatically at a final concentration of 5 μM to avoid known artifacts when used a higher concentrations. NADPH oxidase activity were determined by measuring luminescence over 200 s in a scintillation counter (Lumat LB 9507, Berthold, Germany) in 5-s intervals and was calculated by subtracting the basal values from those in the presence of NADPH. Vessels were then dried, and dry weight was determined. NADPH oxidase activity is expressed as relative luminescence units (RLU)/min/mg dry aortic tissue.

2.4. In situ detection of vascular ROS production

Unfixed thoracic aortic rings were cryopreserved (phosphate buffer solution 0.1 mol/L, PBS, plus 30% sucrose for 1–2 h), included in optimum cutting temperature compound medium (Tissue-Tek; Sakura Finetechnical, Tokyo, Japan), frozen (−80 °C), and 10 μm cross sections were obtained in a cryostat (Microm International Model HM500 OM). Sections were incubated for 30 min in Hepes buffered solution containing dihydroethidium (DHE, 10^{−5} M) (Sigma–Aldrich, Madrid, Spain), counterstained with the nuclear stain 4,6-diamidino-2-phenylindole dichlorohydrate (DAPI, 3 × 10^{−7} M) (Calbiochem, Madrid, Spain) and in the following 24 h examined on a fluorescence microscope (Leica DM IRB, Wetzlar, Germany). Sections were photographed and ethidium and DAPI fluorescence were quantified using ImageJ (version 1.32j, NIH, <http://rsb.info.nih.gov/ij/>). ROS production was estimated from the ratio of ethidium/DAPI fluorescence [37]. In preliminary experiments, before incubation with DHE, serial sections were treated with either the O₂^{•−} scavenger tiron (10 μM), or pegylated

Table 1
Oligonucleotides used for real-time RT-PCR.

mRNA targets	Description	Sense	Antisense
<i>Actb</i>	Beta actin	AATCGTGGCGTACATCAAAG	ATGCCACAGGATCCATACC
<i>p22^{phox}</i>	p22 ^{phox}	GCGGTGTGGACAGAAGTACC	CTTGGGTTTAGGCTCAATGG
<i>NOX-1</i>	NADPH oxidase-1	TCTTGCTGGTTGACACTTGC	TATGGGAGTGGGAATCTTGG
<i>NOX-2</i>	NADPH oxidase-2	ACCAAGTGGTCACTCATCC	TCCAGGCATCTTGAAACTCC
<i>NOX-4</i>	NADPH oxidase-4	ACAGTCTGGCTTACCTTCG	TTCTGGATCCTCATTCTGG
<i>DUOX 1,2</i>	DUOX1,2	CAGGACAAGGAGGAGCTGAC	GCGCTCATTAGGTGAAGG
<i>caveolin-1</i>	caveolin-1	TCTACAAGCCCAACAACAAGG	AGGAAAGAGAGGATGGCAAAG
<i>eNOS</i>	Endothelial nitric oxide synthase	ATGGATGAGCCAACCTCAAGG	TGTCGTGTAATCGGTCTTGC

superoxide dismutase (PEG-SOD, 250 U ml⁻¹) (Sigma–Aldrich, Madrid, Spain) for 30 min at 37 °C.

2.5. Western blotting analysis

Aortic homogenates were run on a sodium dodecyl sulphate (SDS)-polyacrylamide electrophoresis. Proteins were transferred to polyvinylidene difluoride membranes (PVDF) (Millipore, MA, USA), incubated with primary monoclonal mouse anti-eNOS and anti-caveolin-1 antibodies (Transduction Laboratories, San Diego, California, USA), and acetyl-histone-3 (Millipore, MA, USA) overnight and with the correspondent secondary peroxidase conjugated antibodies. Antibody binding was detected by an ECL system (Amersham Pharmacia Biotech, Amersham, UK) and

densitometric analysis was performed using Scion Image-Release Beta 4.02 software (<http://www.scioncorp.com>) [37]. Samples were re-probed for expression of smooth muscle α -actin.

2.6. Reverse transcriptase-polymerase chain reaction (RT-PCR) analysis

Total RNA was extracted from aorta by homogenization and converted to cDNA by standard methods. Polymerase chain reaction was performed with a Techgene thermocycler (Techne, Cambridge, UK). A quantitative real-time RT-PCR technique was used to analyze mRNA expression of caveolin-1, eNOS, p22^{phox}, NOX-4, NOX-1, NOX-2, and Duox 1,2. The sequences of the sense and antisense primers used for amplification (Sigma–Aldrich,

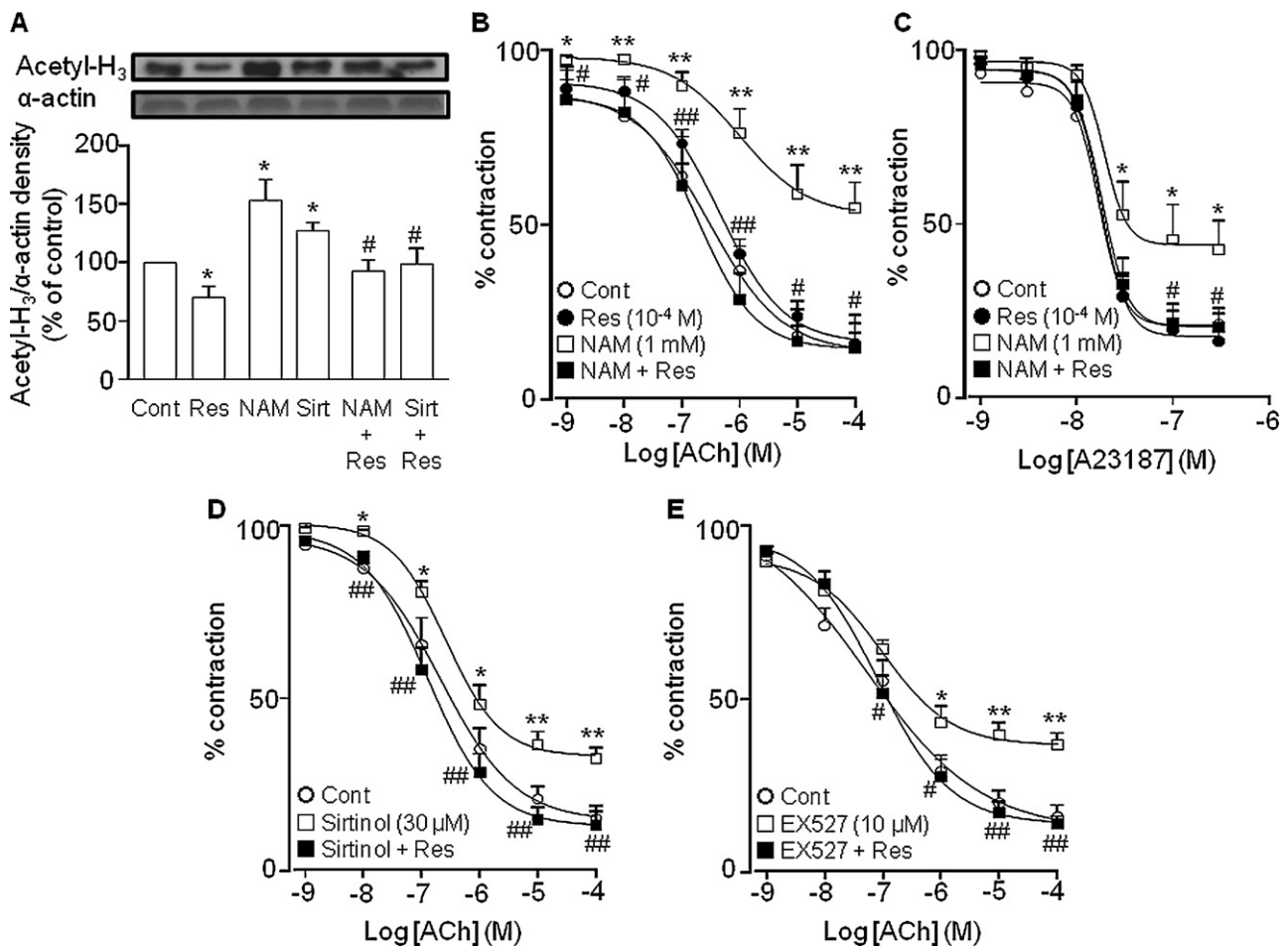


Fig. 1. Effects of SIRT1 inhibition on endothelial function. (A) Effects of the SIRT1 inhibitors NAM and sirtinol on the acetylation of histone-3 (H₃). Panels show representative Western blots and histograms represent densitometric values normalized to the corresponding α -actin. (B–E) Vascular relaxant responses induced by acetylcholine (ACh, B, D and E) and the calcium ionophore (A23187, C) in aortae pre-contracted by 1 μ M phenylephrine (Phe) and preincubated 5 h with or without resveratrol (Res, 100 μ M) and/or nicotinamide (NAM, 1 mM, B and C), or sirtinol (30 μ M, D), or EX527 (10 μ M, E). Values are expressed as mean \pm SEM ($n = 4$ –12 rings from different rats) * $P < 0.05$ and ** $P < 0.01$ as compared to the control group. # $P < 0.05$ and ## $P < 0.01$ as compared to NAM or sirtinol.

Table 2

Vasorelaxing effect of acetylcholine (10^{-9} M to 10^{-4} M) in different experimental conditions in intact rat aortic rings pre-contracted by phenylephrine ($1 \mu\text{M}$).

Experimental group	n	Precontraction (g)	pD ₂	E _{max} (%)
Control	6	1.75 ± 0.20	6.90 ± 0.32	84.9 ± 3.5
Res	8	1.64 ± 0.10	6.52 ± 0.09	83.8 ± 5.8
NAM	12	1.67 ± 0.15	6.06 ± 0.18**	45.2 ± 7.4**
NAM + res	7	1.60 ± 0.13	6.84 ± 0.13*	85.2 ± 9.5#
NAM + SOD	4	1.69 ± 0.11	7.12 ± 0.15##	91.8 ± 1.8##
NAM + apo	8	1.80 ± 0.16	6.85 ± 0.28*	90.9 ± 2.5##
NAM + rot	6	1.91 ± 0.30	6.49 ± 0.33	59.0 ± 6.0
NAM + clof	5	1.76 ± 0.23	7.28 ± 0.36##	81.3 ± 7.5##
NAM + res + GW	6	1.59 ± 0.25	6.62 ± 0.25	72.3 ± 1.7†
Sirt	10	1.90 ± 0.16	6.46 ± 0.27	67.5 ± 3.2**
Sirt + res	9	1.81 ± 0.15	6.94 ± 0.14	86.6 ± 3.8##
Sirt + SOD	9	1.92 ± 0.18	6.81 ± 0.24	85.1 ± 2.9##
EX527	7	1.73 ± 0.19	7.12 ± 0.13	63.4 ± 3.6**
EX527 + res	8	1.64 ± 0.23	7.07 ± 0.10	86.1 ± 2.4##
EX527 + SOD	5	1.80 ± 0.17	7.13 ± 0.07	80.0 ± 2.5##

Res, resveratrol; NAM, nicotinamide; SOD, superoxide dismutase; apo, apocynin; rot, rotenone; clof, clofibrate; GW, GW6471; Sirt, sirtinol. Concentrations of the different drugs used are described in Section 2. Results are expressed as mean ± SEM of *n* experiments.

** *P* < 0.01 vs control.

P < 0.05 vs NAM or Sirt or EX527.

P < 0.01 vs NAM or Sirt or EX527.

† *P* < 0.05 vs NAM + sirt.

Table 3

Vasorelaxing effect of calcium ionophore (A23187, 10^{-9} M to 10^{-6} M) in different experimental conditions in intact rat aortic rings pre-contracted by phenylephrine ($1 \mu\text{M}$).

Experimental group	n	Precontraction (g)	pD ₂	E _{max} (%)
Control	9	1.82 ± 0.29	7.87 ± 0.09	78.8 ± 4.6
Res	8	1.68 ± 0.16	7.74 ± 0.06	83.7 ± 3.5
NAM	10	1.88 ± 0.26	7.58 ± 0.13	57.4 ± 8.3*
NAM + res	8	1.71 ± 0.23	7.68 ± 0.04	79.8 ± 4.1#

Res, resveratrol; NAM, nicotinamide. Concentrations of the different drugs used are described in Section 2. Results are expressed as mean ± SEM of *n* experiments.

* *P* < 0.05 vs control.

P < 0.05 vs NAM.

Madrid, Spain) are described in Table 1. Quantification was performed using the $\Delta\Delta C_t$ method. The housekeeping gene β -actin was used for internal normalization.

2.7. Co-immunoprecipitation

Preparation of nuclear extracts and immunoprecipitation procedures have been described previously [38]. Nuclear extracts were immunoprecipitated by using a PPAR α antibody (Santa Cruz Biotechnology, Inc., Santa Cruz, CA, USA) and analyzed by Western blot using antibodies against SIRT1 (Upstate Biotechnology, Inc., Lake Placid, NY, USA), PGC-1 α (Santa Cruz Biotechnology), and acetylated-lysine (Cell Signaling Technology, Inc., Beverly, MA, USA) antibodies.

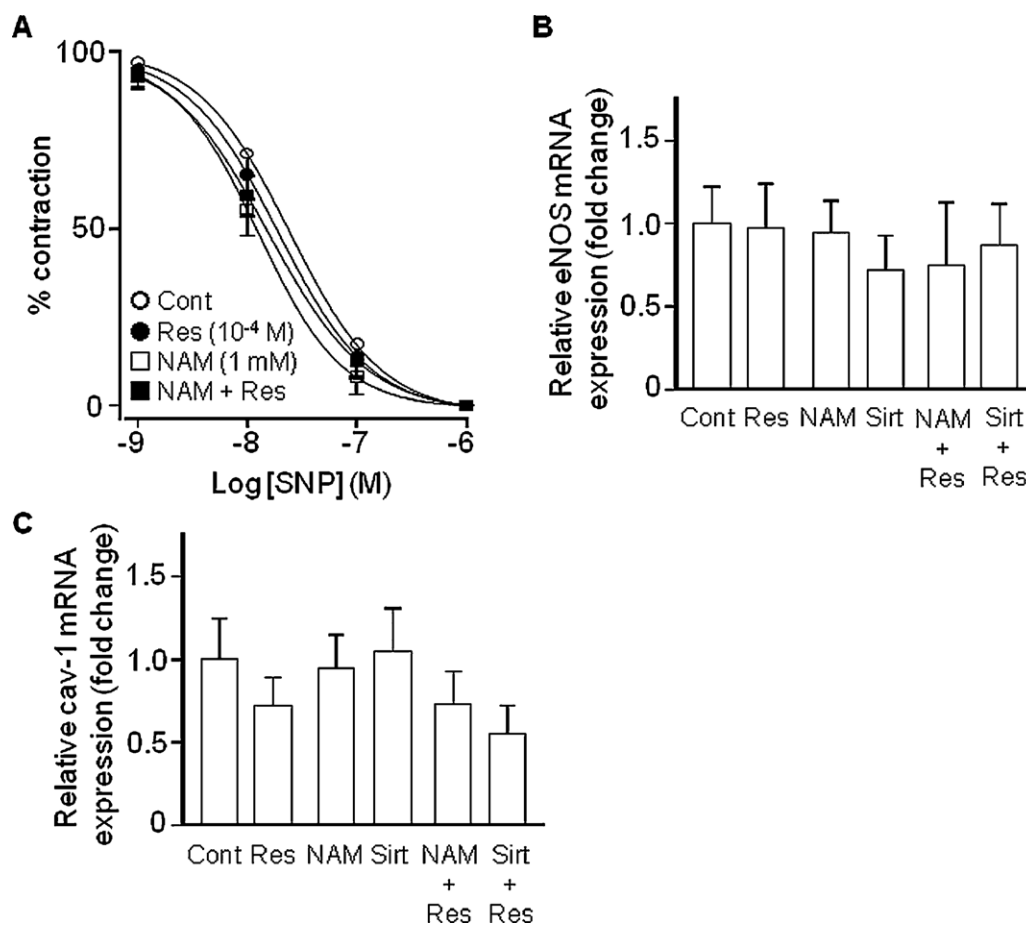


Fig. 2. Effects of SIRT1 inhibition on the NO pathway in the rat aorta. (A) Relaxant responses induced by sodium nitroprusside (SNP) in endothelium-denuded aortae pre-contracted by $1 \mu\text{M}$ Phe preincubated 5 h with or without resveratrol (Res, $100 \mu\text{M}$) and/or nicotinamide (NAM, 1 mM). (B and C) Effects of SIRT1 inhibitors and resveratrol on the mRNA expression of eNOS (B) and caveolin-1 (C) in aortae. Data presented as a ratio of arbitrary units of mRNA ($2^{-\Delta\Delta C_t}$). Values are expressed as mean ± SEM (*n* = 4–8 rings from different rats).

2.8. Statistical analysis

Results are expressed as mean \pm SEM and n reflects the number of experiments performed. Concentration–response curves were fitted to a logistic equation and from these plots the maximal relaxant effect (E_{max}) and the negative logarithm of the concentration producing half maximal relaxation (pD_2) were calculated. Statistically significant differences between groups were calculated by an analysis of variance (ANOVA) followed by a Newman–Keuls test. $P < 0.05$ was considered statistically significant. When the overall difference was significant comparisons were made using Bonferroni's method with an appropriate error. Analysis of the nested design was also carried out with groups and concentrations to compare the concentration–response curves to ACh. The remaining variables were compared using a two-way factor design, where group and treatment were fixed effect factors with unequal sample sizes in the different groups. When interaction was significant Bonferroni's method was used for pairwise comparisons. $P < 0.05$ was considered statistically significant.

3. Results

3.1. SIRT1 inhibition impairs endothelium-dependent aortic rings relaxation

The acetylation of histone-3 protein was reduced in aortic rings incubated for 5 h with resveratrol and increased with either NAM or sirtinol. The increase in histone-3 acetylation induced by both SIRT1 inhibitors was prevented coinubcation with resveratrol (Fig. 1A).

Incubation of the aortic rings for 5 h in the presence of the SIRT1 inhibitors NAM, sirtinol, or EX527 produced no significant changes in the contractile response to phenylephrine (1 μ M) (Tables 2 and 3). However, NAM (Table 2, Fig. 1B and C), sirtinol (Table 3, Fig. 1D), and EX527 (Table 2, Fig. 5E) led to the development of endothelial dysfunction as indicated by the reduction in both the sensitivity (pD_2) and maximal relaxant effect of ACh (Table 2) and maximal relaxation of A23187 (Table 3) induced by NAM, and reduction of maximal relaxant effect of ACh induced by both sirtinol and EX527 (Table 2). Incubation with resveratrol alone did not modify the

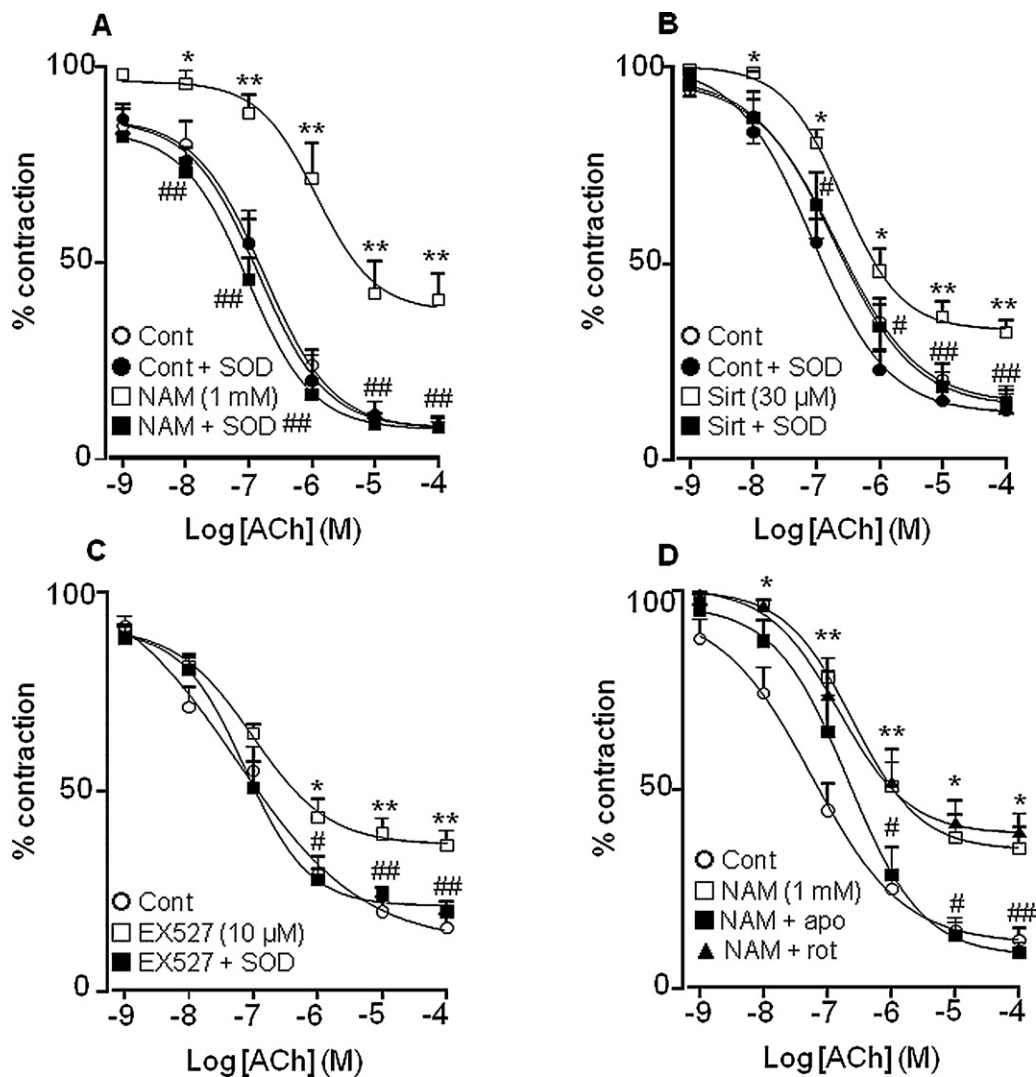


Fig. 3. Role of superoxide on endothelial dysfunction induced by SIRT1 inhibition. Relaxant responses induced by acetylcholine (ACh) in aortae pre-contracted by 1 μ M phenylephrine (Phe) and preincubated 5 h with nicotinamide (NAM, 1 mM, A and D) or sirtinol (Sirt, 30 μ M, B), or EX527 (10 μ M, C) and in the presence or the absence of SOD (100 U/mL) 30 min before the addition of Phe, or in the presence of rotenone (rot, 5 μ M) or apocynin (apo, 100 μ M) during the incubation period with NAM (C). Values are expressed as mean \pm SEM ($n = 6$ –8 rings from different rats). * $P < 0.05$ and ** $P < 0.01$ as compared to the control group. # $P < 0.05$ and ## $P < 0.01$ as compared to NAM or Sirt or Ex527 groups.

relaxant effect of ACh but prevented the endothelial dysfunction induced by NAM, sirtinol, and EX527.

3.2. SIRT1 activity has no influence on either the responsiveness of the NO-cGMP pathway or the eNOS and caveolin expression

In contrast to the results with ACh, the endothelium independent vasodilation induced by the NO donor sodium nitroprusside was similar in rings incubated with ($pD_2 = 7.94 \pm 0.12$ and $E_{max} = 101.0 \pm 1.2$, $n = 7$) or without NAM ($pD_2 = 7.74 \pm 0.13$ and $E_{max} = 99.6 \pm 1.1$, $n = 11$) and in the presence or in the absence of resveratrol (Fig. 2A). Gene expression of eNOS (Fig. 2B) and caveolin-1 (Fig. 2C), an allosteric negative regulator of eNOS, were unchanged by SIRT1 inhibition.

3.3. Role of ROS and NADPH oxidase on endothelial dysfunction induced by SIRT1 inhibition

The impaired relaxant response to ACh induced by NAM, sirtinol, or EX527 was restored by the presence of the $O_2^{\cdot-}$ scavenger SOD in the bath (Fig. 3A–C, Table 2). However, rotenone, a mitochondrial complex I inhibitor, was unable to prevent endothelial dysfunction induced by NAM (Fig. 3D, Table 2). Since NADPH oxidase is the major source of $O_2^{\cdot-}$ in the vascular wall, we studied the effects of the NADPH oxidase inhibitor apocynin. This drug also increased ACh relaxation in arteries preincubated with NAM (Fig. 3D, Table 2). Moreover, ROS production (Fig. 4A) and

NADPH oxidase activity (Fig. 4B) were increased by NAM and these effects were abolished by apocynin. The mRNA expression of the NADPH oxidase subunits p22^{phox} and NOX4 (Fig. 4C) were also increased by NAM and sirtinol and were suppressed by coinubation with resveratrol. However, mRNA levels of NOX-1, NOX-2 and Duox 1,2 were similar in all experimental groups (Fig. 4C).

3.4. The protective effects of resveratrol on endothelial dysfunction induced by SIRT1 inhibition require an active PPAR α pathway

The improvement in relaxant response to ACh (Fig. 5A, Table 2) and the reduction in both p22^{phox} (Fig. 5C) and NOX4 (Fig. 5D) expression induced by resveratrol in NAM incubated rings were suppressed by coinubation with the PPAR α antagonist GW6471. Moreover, the PPAR α agonist clofibrate exhibited similar protective effects than resveratrol in the preventing NAM-induced impairment of ACh relaxation (Fig. 5B, Table 2) and overexpression of p22^{phox} (Fig. 5C) or NOX4 (Fig. 5D) expression. Collectively, these findings suggest that endothelial dysfunction induced by SIRT1 inhibition is related with an impairment of PPAR α pathway in aortic rings.

3.5. SIRT1 interacts with PPAR α and regulates PGC-1 α acetylation

In PPAR α immunoprecipitates from aortic ring extracts, Western blotting detected SIRT1 (Fig. 6A) indicating an interaction between both proteins. Because SIRT1 acts as a protein deacetylase, we explored the relationship between SIRT1 and PPAR α

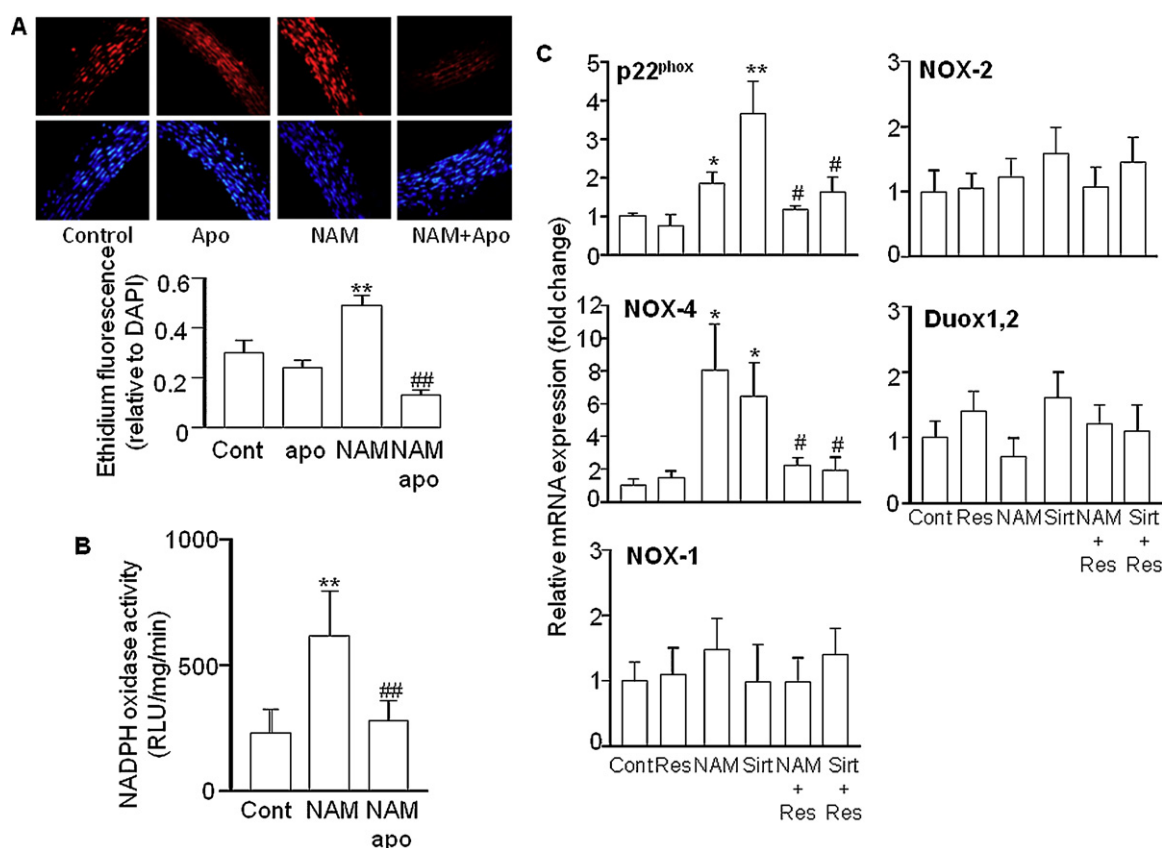


Fig. 4. Role of NADPH oxidase pathway on endothelial dysfunction induced by SIRT1 inhibition. (A) Effects of nicotinamide (NAM, 1 mM) and apocynin (apo, 100 μ M) on the in situ ROS production. Top pictures show arteries incubated in the presence of DHE which produces a red fluorescence when oxidized by ROS and bottom pictures show the blue fluorescence of the nuclear stain DAPI ($\times 400$ magnification). Averaged values, mean \pm SEM ($n = 5-7$ rings from different rats) of the red fluorescence normalized to the blue DAPI fluorescence. (B) NADPH oxidase activity measured by lucigenin-enhanced chemiluminescence in aortae preincubated with NAM and/or apo. (C) Expression of NADPH oxidase subunits p22^{phox}, NOX4, NOX1, NOX2, and Duox 1,2 at the level of mRNA by RT-PCR in aortae preincubated with SIRT1 inhibitors NAM or sirtinol (Sirt, 30 μ M) and in the presence or the absence of resveratrol (Resv, 100 μ M). Data presented as a ratio of arbitrary units of mRNA ($2^{-\Delta\Delta C_t}$) normalized to the corresponding RT-PCR products of β -actin. Values are expressed as mean \pm SEM ($n = 6-8$ rings from different rats). * $P < 0.05$ and ** $P < 0.01$ as compared to the control group. # $P < 0.05$ and ### $P < 0.01$ as compared to NAM or sirt. (For interpretation of the references to color in this figure legend, the reader is referred to the web version of this article.)

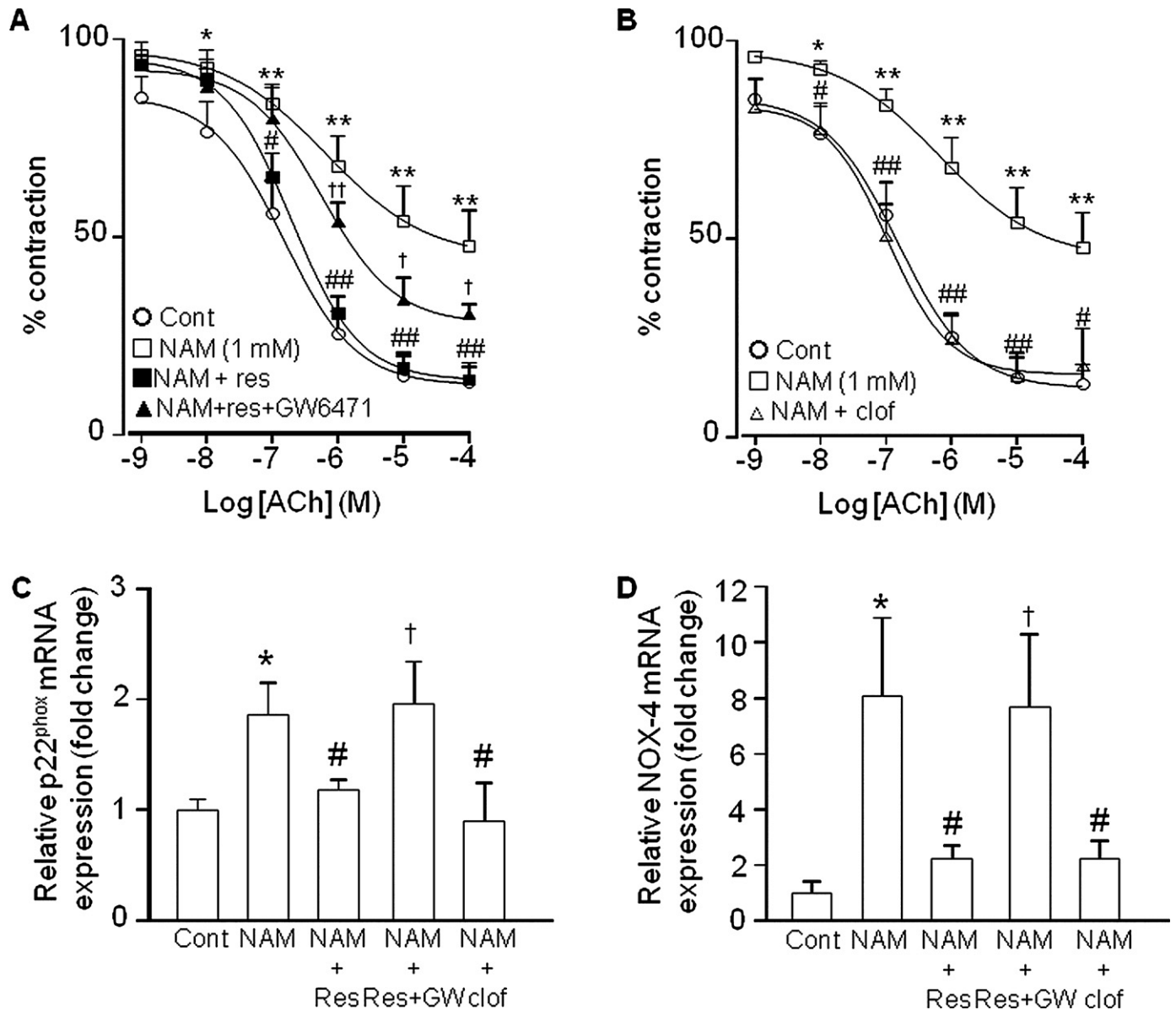


Fig. 5. Role of PPAR α on endothelial dysfunction induced by SIRT1 inhibition. (A and B) Relaxant responses induced by acetylcholine (ACh) in aortae pre-contracted by 1 μ M phenylephrine (Phe) and preincubated 5 h with nicotinamide (NAM, 1 mM) and/or resveratrol (Res, 100 μ M) and/or the PPAR α antagonist, GW6471 (1 μ M, A) or with the PPAR α agonist, clofibrate (Clof, 1 μ M). Expression of NADPH oxidase subunits p22^{phox} (C) and NOX4 (D) at the level of mRNA by RT-PCR in aortae preincubated with NAM and in the presence or the absence of resv and with GW6471 (GW) or clof. Data presented as a ratio of arbitrary units of mRNA ($2^{-\Delta\Delta C_t}$) normalized to the corresponding RT-PCR products of β -actin. Values are expressed as mean \pm SEM ($n = 6$ –8 rings from different rats). * $P < 0.05$ and ** $P < 0.01$ as compared to the control group. * $P < 0.05$ and ** $P < 0.01$ as compared to NAM † $P < 0.05$ and †† $P < 0.01$ as compared to NAM + Res.

activity by analyzing the acetylation status of PGC-1 α (Fig. 6B and D), a major co-activator of PPAR α known to be expressed in the vascular wall and target of deacetylation by SIRT1 in other cell systems [39]. No changes were observed in PGC-1 α levels in immunoprecipitates of nuclear extracts of aortic rings with PPAR α antibody, either treated or untreated with NAM or resveratrol (Fig. 6C). However, SIRT1 inhibition with NAM or activation with resveratrol resulted in a marked increase and decrease, respectively, in the signal corresponding to lysine acetylation of PGC-1 α in the immunoprecipitate.

4. Discussion

In the present study we demonstrate that inhibition of SIRT1 induces endothelial dysfunction via upregulation of the NADPH oxidase subunits, p22^{phox} and NOX4, resulting in an increased vascular O₂^{•-} production. We propose a model in which SIRT1

inhibition favors the acetylation of PGC-1 α , repressing PPAR α activity.

The endothelial dysfunction observed using pharmacological SIRT1 inhibitors confirms previous observations in rat aortic rings in which inhibition of endogenous SIRT1 was achieved by a dominant negative SIRT1 mutant adenovirally expressed in the endothelium [33]. Our results are also consistent with the fact that a reduction in SIRT1 expression and activity in arteries from aged rodents and humans is associated with impairment of NO-dependent relaxation [30–32].

Sirtuins may play a critical role in endothelial homeostasis. In agreement with previous reports [33,39], our data shows that eNOS mRNA was not downregulated after SIRT1 inhibition, and we also found that caveolin-1 mRNA, an allosteric negative regulator of eNOS, was unchanged by SIRT1 inhibition. Moreover, changes in the sensibility to the NO-cGMP pathway in vascular smooth muscle cells were ruled out since the relaxant responses to the

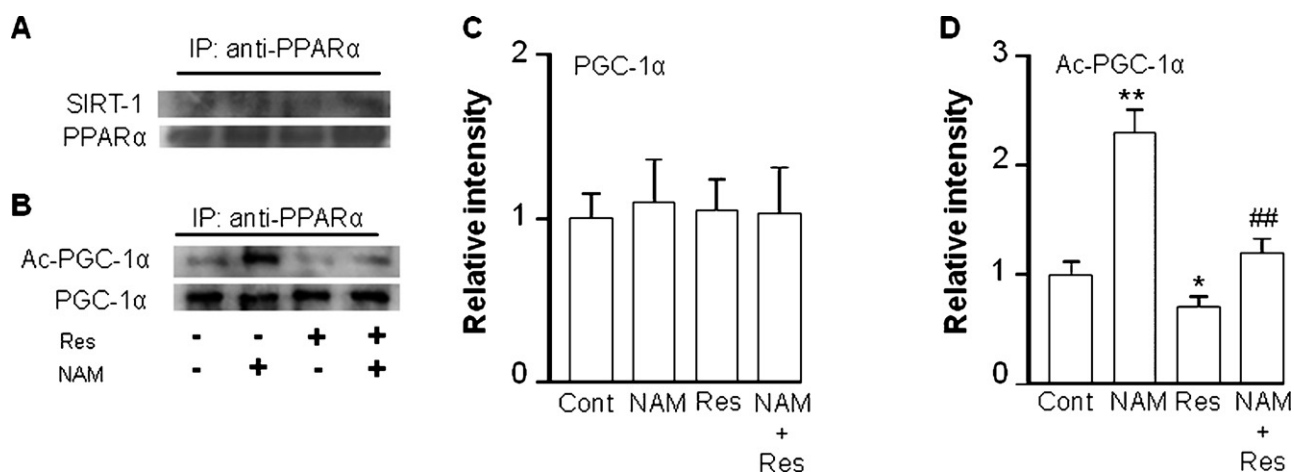


Fig. 6. Interactions between SIRT1 and PPAR α and PGC-1 α acetylation after SIRT1 inhibition. Immunoblots of precipitated anti-PPAR α probed with (A) SIRT1, (B) PGC-1 α and acetylated-PGC-1 α antibodies in aortae preincubated with 5 h with nicotinamide (NAM, 1 mM) and/or resveratrol (Res, 100 μ M). (C and D) Averaged densitometric values of PGC-1 α and acetylated-PGC-1 α bands. * P < 0.05 and ** P < 0.01 as compared to the control group. ## P < 0.01 as compared to NAM.

endothelium-independent NO-donor sodium nitroprusside were not modified [present results and 33]. SIRT1 has been shown to bind eNOS and regulate its post-transcriptional activation. Over-expression of SIRT1 deacetylates lysines 496 and 506 in the calmodulin-binding domain of eNOS leading to enhance NO production [33,40]. Therefore, the mechanism proposed for endothelial dysfunction after SIRT1 inhibition involves an increased acetylation of eNOS leading to decreased enzyme activity. This was supported by a decreased NO production after transfection of SIRT1 RNAi but not by unchanged NO production in the catalytically inactive dominant negative SIRT1 mutant [33]. Herein, we demonstrate an additional mechanism which, besides changes in the eNOS enzyme activity, involves an increased NO inactivation by NADPH oxidase-derived $O_2^{\bullet-}$. This is consistent with the implication of increased NO degradation by $O_2^{\bullet-}$ as a key mechanism for age-related endothelial dysfunction [8–15].

It is well established that $O_2^{\bullet-}$ rapidly inactivates NO and it is a major contributor to the onset and development of endothelial dysfunction [41]. We found for the first time that the impaired ACh-evoked endothelial dependent relaxations induced by both SIRT1 and SIRT2 inhibitors, NAM and sirtinol, and by the selective SIRT1 inhibitor EX527 were suppressed by the presence of SOD in the bath, indicating a principal role of $O_2^{\bullet-}$ in the development of endothelial dysfunction. Moreover, several results support the role of NADPH oxidase as a major source of $O_2^{\bullet-}$ involved in endothelial dysfunction induced by SIRT1 inhibition. First, SIRT1 inhibition by NAM increased ROS levels and NADPH oxidase activity, which were suppressed by coincubation with the NADPH oxidase inhibitor apocynin. Second, NAM and sirtinol enhanced the expression of the catalytic and the regulatory subunits, NOX-4 and p22^{phox}, respectively, of the NADPH oxidase system and these effects were prevented by coincubation with the SIRT1 activator resveratrol, showing that the main source of $O_2^{\bullet-}$ in the vasculature is also controlled by SIRT1. Our results are consistent with previous evidences [34–36] in endothelial and vascular smooth muscle cells which found that reducing SIRT1 activity resulted in an increased ROS production and NADPH oxidase subunits over-expression in vascular cells. Third, inhibition of NADPH oxidase activity with apocynin prevented the impairment of ACh relaxations induced by NAM. Despite these evidences we cannot fully rule out that the mitochondria are involved. In fact, NADPH oxidase induction might occur as a consequence of mitochondrial stress [42]. However, the impaired ACh relaxation induced by NAM seemed to be independent of mitochondrial ROS production through the mitochondrial complex I, since the inhibitor rotenone did not improve this relaxant response.

A number of proteins are targeted by SIRT1 for deacetylation including transcription factors, transcriptional cofactors and chromatin modifying enzymes (e.g. p53, Foxo, NCoR/SMRT, PGC-1 α or SUV39H1) which mediate specific SIRT1-dependent cellular responses [39]. PGC-1 α is a major co-activator of PPAR α known to be expressed in the vascular wall [43]. PPAR α agonists decreased NADPH oxidase-driving $O_2^{\bullet-}$ production in several conditions such as hypertension, diabetes or hyperlipidemia [44–47]. In this study, we demonstrated the formation of a complex involving PPAR α and SIRT1 in the rat aorta. The observation that SIRT1 inhibition promotes the acetylated status of PGC-1 α , which reduces PPAR α activity, provides an explanation for the enhanced expression of NADPH oxidase subunits. In fact, we found that the protective effects of the SIRT1 activator resveratrol on endothelial dysfunction induced by SIRT1 inhibition were prevented after coincubation with the PPAR α antagonist GW6471. Likewise, the protective effects of SIRT1 over-expression on fatty acid oxidation genes, proinflammatory marker MCP-1 [48], and cardiac hypertrophy [49] were lost after PPAR α inhibition, indicating that PPAR α is a common factor that regulates these diverse processes. Moreover, the PPAR α agonist clofibrate inhibited the over-expression of NADPH oxidase subunits and the endothelial dysfunction induced by SIRT1 inhibition. Thus, the nuclear factor PPAR α seems to be a critical factor linking SIRT1 inhibition with the processes of oxidative stress and endothelial dysfunction.

From a biomedical viewpoint, the possibility of stopping or reversing aging-associated endothelial dysfunction resulting of low SIRT1 expression, and thereby slowing atherosclerosis, is a topic of considerable interest. Collectively, the findings reported in this study suggest that the convergence of SIRT1 and PPAR α pathways in the vessel wall increases the relevance of PPAR α agonists in preventing endothelial dysfunction in aging. Very recently it has been described that PPAR α could improve endothelial vasodilation in humans presenting endothelial dysfunction, but this was not applicable to aged vessels [50]. The reason for this loss in the response to PPAR α activation with aging might be related to the short duration of exposure (25 min) of the vessels to the PPAR α agonist, insufficient for the genomic effects of nuclear receptors.

In conclusion, we demonstrated that pharmacological inhibition of SIRT1 induces endothelial dysfunction. This confirms previous studies based on a dominant negative SIRT1 mutant adenovirally expressed in the endothelium. Besides the increased acetylation and reduced eNOS activity previously reported, we present evidences for an additional mechanism for this process which involves an increased PGC-1 α acetylation and the

subsequent PPAR α inhibition. This results in upregulation of the NADPH oxidase subunits p22^{phox} and NOX4 and increased NADPH oxidase-driven O₂^{•-} production. The unpaired endothelial function as well as the overexpression of NADPH oxidase subunits could be restored by the SIRT1 activator resveratrol or by the PPAR α agonist clofibrate.

Acknowledgments

This work was supported by grants from Comisión Interministerial de Ciencia y Tecnología (SAF2011-28150, SAF2010-22066-CO2-01 and -02) and by Ministerio de Economía y Competitividad, Instituto de Salud Carlos III (Red HERACLES RD06/0009), Spain. M.J.Z. and M.S. are holders of studentships from Spanish Ministry of Science and Education and M.R. is partially supported by a grant from Ministerio de Ciencia e Innovación Campus de Excelencia Internacional (Programa GREIB), Spain.

References

- Celermajer DS, Sorensen KE, Bull C, Robinson J, Deanfield JE. Endothelium-dependent dilation in the systemic arteries of asymptomatic subjects relates to coronary risk factors and their interaction. *J Am Coll Cardiol* 1994;24:1468–74.
- Taddei S, Virdis A, Ghiadoni L, Mattei P, Sudano I, Bernini G, et al. Menopause is associated with endothelial dysfunction in women. *Hypertension* 1996;28:576–82.
- Spier SA, Delp MD, Meininger CJ, Donato AJ, Ramsey MW, Muller-Delp JM. Effects of ageing and exercise training on endothelium-dependent vasodilatation and structure of rat skeletal muscle arterioles. *J Physiol* 2004;556:947–58.
- Lesniewski LA, Connell ML, Durrant JR, Foliari BJ, Anderson MC, Donato AJ, et al. B6D2F1 mice are a suitable model of oxidative stress-mediated impaired endothelium-dependent dilation with aging. *J Gerontol A Biol Sci Med Sci* 2009;64:9–20.
- Seals DR, Jablonski KL, Donato AJ. Aging and vascular endothelial function in humans. *Clin Sci (Lond)* 2011;120:357–75.
- Yeboah J, Crouse JR, Hsu FC, Burke GL, Herrington DM. Brachial flow-mediated dilation predicts incident cardiovascular events in older adults: the Cardiovascular Health Study. *Circulation* 2007;115:2390–7.
- Lind L, Berglund L, Larsson A, Sundström J. Endothelial function in resistance and conduit arteries and 5-year risk of cardiovascular disease. *Circulation* 2011;123:1545–51.
- van der Loo B, Labugger R, Skepper JN, Bachschmid M, Kilo J, Powell JM, et al. Enhanced peroxynitrite formation is associated with vascular aging. *J Exp Med* 2000;192:1731–44.
- Taddei S, Virdis A, Ghiadoni L, Salvetti G, Bernini G, Magagna A, et al. Age-related reduction of NO availability and oxidative stress in humans. *Hypertension* 2001;38:274–9.
- Fleming I, Busse R. NO: the primary EDRF. *J Mol Cell Cardiol* 1999;31:5–14.
- Csiszar A, Ungvari Z, Edwards JG, Kaminski P, Wolin MS, Koller A, et al. Aging-induced phenotypic changes and oxidative stress impair coronary arteriolar function. *Circ Res* 2002;90:1159–66.
- Donato AJ, Eskurza I, Silver AE, Levy AS, Pierce GL, Gates PE, et al. Direct evidence of endothelial oxidative stress with aging in humans: relation to impaired endothelium-dependent dilation and upregulation of nuclear factor-kappaB. *Circ Res* 2007;100:1659–66.
- Smith AR, Visioli F, Hagen TM. Plasma membrane-associated endothelial nitric oxide synthase and activity in aging rat aortic vascular endothelia markedly decline with age. *Arch Biochem Biophys* 2006;454:100–5.
- Soucy KG, Ryou S, Benjo A, Lim HK, Gupta G, Sohi JS, et al. Impaired shear stress-induced nitric oxide production through decreased NOS phosphorylation contributes to age-related vascular stiffness. *J Appl Physiol* 2006;101:1751–9.
- Trott DW, Gunduz F, Laughlin MH, Woodman CR. Exercise training reverses age-related decrements in endothelium-dependent dilation in skeletal muscle feed arteries. *J Appl Physiol* 2009;106:1925–34.
- Trott DW, Seawright JW, Luttrell MJ, Woodman CR. NAD(P)H oxidase-derived reactive oxygen species contribute to age-related impairments of endothelium-dependent dilation in rat soleus feed arteries. *J Appl Physiol* 2011;110:1171–80.
- Pierce GL, Donato AJ, LaRocca TJ, Eskurza I, Silver AE, Seals DR. Habitually exercising older men do not demonstrate age-associated vascular endothelial oxidative stress. *Aging Cell* 2011;10:1032–7.
- Eskurza I, Monahan KD, Robinson JA, Seals DR. Effect of acute and chronic ascorbic acid on flow-mediated dilatation with sedentary and physically active human ageing. *J Physiol* 2004;556:315–24.
- Kirby BS, Voyles WF, Simpson CB, Carlson RE, Schrage WG, Dinenna FA. Endothelium-dependent vasodilatation and exercise hyperaemia in ageing humans: impact of acute ascorbic acid administration. *J Physiol* 2009;587:1989–2003.
- Chen D, Steele AD, Lindquist S, Guarente L. Increase in activity during calorie restriction requires sirt1. *Science* 2005;310:1641.
- Li Y, Xu W, McBurney MW, Longo VD. Sirt1 inhibition reduces igf-1/irs-2/ras/erk1/2 signaling and protects neurons. *Cell Metab* 2008;8:38–48.
- Oberdoerffer P, Michan S, McVay M, Mostoslavsky R, Vann J, Park SK, et al. Sirt1 redistribution on chromatin promotes genomic stability but alters gene expression during aging. *Cell* 2008;135:907–18.
- Yu J, Auwerx J. Protein deacetylation by sirt1: an emerging key post-translational modification in metabolic regulation. *Pharmacol Res* 2010;62:35–41.
- Lin SJ, Defossez PA, Guarente L. Requirement of nad and sir2 for life-span extension by calorie restriction in *Saccharomyces cerevisiae*. *Science* 2000;289:2126–8.
- Rogina B, Helfand SL. Sir2 mediates longevity in the fly through a pathway related to calorie restriction. *Proc Natl Acad Sci USA* 2004;101:15998–6003.
- Wang Y, Tissenbaum HA. Overlapping and distinct functions for a *Caenorhabditis elegans* sir2 and daf-16/foxo. *Mech Ageing Dev* 2006;127:48–56.
- Greer EL, Brunet A. Different dietary restriction regimens extend lifespan by both independent and overlapping genetic pathways in *C. elegans*. *Aging Cell* 2009;8:113–27.
- Kaeblerlein M, Kirkland KT, Fields S, Kennedy BK. Sir2-independent life span extension by calorie restriction in yeast. *PLoS Biol* 2004;2:E296.
- Ungvari Z, Kaley G, de Cabo R, Sonntag WE, Csiszar A. Mechanisms of vascular aging: new perspectives. *J Gerontol A Biol Sci Med Sci* 2010;65:1028–41.
- Ungvari Z, Parrado-Fernandez C, Csiszar A, de Cabo R. Mechanisms underlying caloric restriction and lifespan regulation: implications for vascular aging. *Circ Res* 2008;102:519–28.
- Rippe C, Lesniewski L, Connell M, LaRocca T, Donato A, Seals D. Short-term calorie restriction reverses vascular endothelial dysfunction in old mice by increasing nitric oxide and reducing oxidative stress. *Aging Cell* 2010;9:304–12.
- Donato AJ, Magerko KA, Lawson BR, Durrant JR, Lesniewski LA, Seals DR. SIRT-1 and vascular endothelial dysfunction with ageing in mice and humans. *J Physiol* 2011;589:4545–54.
- Mattagajasingh I, Kim CS, Naqvi A, Yamamori T, Hoffman TA, Jung SB, et al. SIRT1 promotes endothelium-dependent vascular relaxation by activating endothelial nitric oxide synthase. *Proc Natl Acad Sci USA* 2007;104:14855–60.
- Kao CL, Chen LK, Chang YL, Yung MC, Hsu CC, Chen YC, et al. Resveratrol protects human endothelium from H(2)O(2)-induced oxidative stress and senescence via SirT1 activation. *J Atheroscler Thromb* 2010;17:970–9.
- Hori YS, Kuno A, Hosoda R, Tanno M, Miura T, Shimamoto K, et al. Resveratrol ameliorates muscular pathology in the dystrophic mdx mouse, a model for Duchenne muscular dystrophy. *J Pharmacol Exp Ther* 2011;338:784–94.
- Li L, Gao P, Zhang H, Chen H, Zheng W, Lv X, et al. SIRT1 inhibits angiotensin II-induced vascular smooth muscle cell hypertrophy. *Acta Biochim Biophys Sin (Shanghai)* 2011;43:103–9.
- Zarzuelo MJ, Jiménez R, Galindo P, Sánchez M, Nieto A, Romero M, et al. Antihypertensive effects of peroxisome proliferator-activated receptor- β activation in spontaneously hypertensive rats. *Hypertension* 2011;58:733–43.
- Planavila A, Laguna JC, Vazquez-Carrera M. Nuclear factor-kappaB activation leads to down-regulation of fatty acid oxidation during cardiac hypertrophy. *J Biol Chem* 2005;280:17464–71.
- Potente M, Dimmeler S. Emerging roles of SIRT1 in vascular endothelial homeostasis. *Cell Cycle* 2008;7:2117–22.
- Ota H, Eto M, Kano MR, Kahyo T, Setou M, Ogawa S, et al. Induction of endothelial nitric oxide synthase, SIRT1, and catalase by statins inhibits endothelial senescence through the Akt pathway. *Arterioscler Thromb Vasc Biol* 2010;30:2205–11.
- Cai H, Harrison DG. Endothelial dysfunction in cardiovascular diseases: the role of oxidant stress. *Circ Res* 2000;87:840–4.
- Wosniak Jr J, Santos CX, Kowaltowski AJ, Laurindo FR. Cross-talk between mitochondria and NADPH oxidase: effects of mild mitochondrial dysfunction on angiotensin II-mediated increase in Nox isoform expression and activity in vascular smooth muscle cells. *Antioxid Redox Signal* 2009;11:1265–78.
- Rodgers JT, Lerin C, Haas W, Gygi SP, Spiegelman BM, Puigserver P. Nutrient control of glucose homeostasis through a complex of PGC-1 α and SIRT1. *Nature* 2005;434:113–8.
- Iglarz M, Touyz RM, Amiri F, Lavoie MF, Diep QN, Schiffrin EL. Effect of peroxisome proliferator-activated receptor- α and - γ activators on vascular remodeling in endothelin-dependent hypertension. *Arterioscler Thromb Vasc Biol* 2003;23:45–51.
- Newaz M, Blanton A, Fidelis P, Oyekan A. NAD(P)H oxidase/nitric oxide interactions in peroxisome proliferator activated receptor (PPAR) α -mediated cardiovascular effects. *Mutat Res* 2005;579:163–71.
- Olukman M, Sezer ED, Ulker S, Sözmén EY, Cinar GM. Fenofibrate treatment enhances antioxidant status and attenuates endothelial dysfunction in streptozotocin-induced diabetic rats. *Exp Diabetes Res* 2010;2010:828531.
- Wang G, He L, Liu J, Yu J, Feng X, Li F, et al. Coronary flow velocity reserve is improved by PPAR- α agonist fenofibrate in patients with hypertriglyceridemia. *Cardiovasc Ther* 2012;361:321–8.
- Rodgers JT, Lerin C, Gerhart-Hines Z, Puigserver P. Metabolic adaptations through the PGC-1 α and SIRT1 pathways. *FEBS Lett* 2008;582:46–53.
- Planavila A, Iglesias R, Giral M, Villarroya F. Sirt1 acts in association with PPAR α to protect the heart from hypertrophy, metabolic dysregulation, and inflammation. *Cardiovasc Res* 2011;90:276–84.
- Angulo J, Vallejo S, El Assar M, García-Septiem J, Sánchez-Ferrer CF, Rodríguez-Mañas L. Age-related differences in the effects of α and γ peroxisome proliferator-activated receptor subtype agonists on endothelial vasodilation in human microvessels. *Exp Gerontol* 2012;47:734–40.